Finite Element Modeling of Transient Eddy Currents in Multilayer Aluminum Structures

Vijay Babbar* and Thomas Krause
Royal Military College of Canada
*Corresponding author: Physics Department, Royal Military College of Canada, Kingston, ON, K7K 7B4, Vijay.Babbar@rmc.ca

Abstract: Transient eddy current (TEC) technique is being developed for detection of flaws located at depth within multilayer aluminum structures. It uses a transient signal to induce eddy currents, which interact with flaws in a conducting structure to produce an output signal that provides information about the flaw. The technique involves designing of a transmit/receive probe to produce an output signal that depends on various parameters, such as number of turns, spacing between the coils, length of the core, etc. The present work involves finite element modeling using COMSOL3.4 Multiphysics software to simulate different types of probes by changing some of these parameters in an attempt to generate an output signal of optimum magnitude and shape. Some of the model results are compared with experimental results from an identical probe configuration and there is, in general, a good agreement. The modeling has also contributed towards understanding of the TEC phenomenon.

Keywords: Transient Eddy Current, Pulsed Eddy Current, Electromagnetic Modeling, Transient Electromagnetic Fields

1. Introduction

Transient eddy current (TEC), also called pulsed eddy current (PEC), is an emerging nondestructive technique that employs a pulsed excitation to induce a transient electromagnetic response from defects lying deep within a conducting structure, such as inner layers of airplane wings [1-5]. Such defects are difficult to inspect by conventional techniques, such as eddy current or ultrasonics. A number of publications on this subject are aimed at a theoretical understanding of the phenomenon, development of appropriate probes, improvements in experimental test systems, and finite element (FE) modeling of the input and output signals [6-8]. The authors recently demonstrated the success of FE modeling, using COMSOL commercial software, by modeling coaxial reflection-type probes to simulate input and output signals that matched closely with those obtained from the experiments employing identical parameters [9]. The present work uses FE modeling to investigate the effect of probe position with respect to defect location on the TEC signal for a flat reflection-type probe. It also investigates the effect of modifying some of the probe design parameters, such as number of turns of the driver and length and permeability of the ferrite core on the output signal.

2. Experimental Details

The circuit diagram of a typical reflection-type probe used for experimental work as well as FE modeling is shown in Fig. 1. The primary circuit consists of a driver of resistance R_{PC} connected in series with a source of emf ε and internal resistance R_{IN} of 53 Ω. The driver current is determined by connecting an additional series resistance R_{PV} of 2 Ω and measuring the voltage across it. The secondary circuit contains a pickup coil of resistance R_{SC} that is coaxially coupled to the driver and connected across an external load of 51 Ω. The coil dimensions and circuit parameters are listed in Table 1. The measurements were made on a stack of aluminum plates, each of dimensions 200 mm × 200 mm × 0.40 mm, with the lower-most plate having a hole of diameter 5 mm. To eliminate the air gaps between the plates, the stack was placed inside a plastic bag attached to a vacuum pump. The minimum lift-off of the probe from the sample surface was 0.23 mm.

3. Finite Element Modeling

COMSOL Multiphysics 3.4 commercial soft-ware was used for FE modeling. We used both two-dimensional (2D) and three-dimensional (3D) models depending on the geometry of the sample as well as the probe. For example, a 2D model was employed to model a ‘no defect’

sample geometry that was used to study the effect of probe lift-off. For geometries involving localized defects, such as circular holes, the 3D half-models were used. Models were produced for a number of plates varying from 0 (air case) to 10, each of thickness 0.4 mm. There was no air gap between the plates, so the plate region was essentially a continuum.

The software uses a smoothed Heaviside step function to generate a square voltage pulse similar to the one produced by experimental pulse generator [8]. The step function is expressed as *flc2hs*(*x*, *s*) and it smoothes within the interval $-s < x < s$. The value of *s* parameter as determined from the experiment and used in the models is 5×10^{-7} s. The typical shape of the step-function for *s* equal to 0.1 is shown in Fig. 2. Only the first half of the pulse is used in models. The time varies from 0 to 2.85×10^{-4} s in steps of 2×10^{-7} s. The Direct (UMFPACK) linear solver is employed to solve the model in the transient analysis mode using Lagrange-Quadratic type of elements.

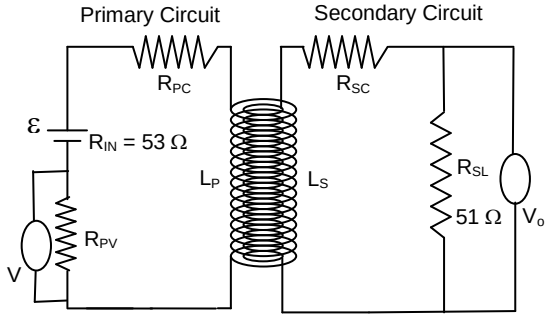

Figure 1. Circuit diagram of the probe used for experimental work as well as finite element modeling.

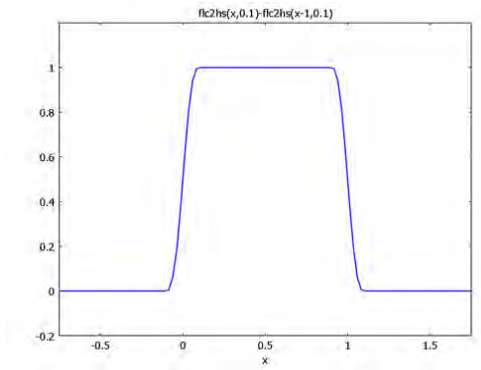

Figure 2. Typical smoothed Heaviside step-function for s = 0.1. The modeled value of s was 5×10^{-7} s.

4. 'No Defect' Models

A 2D quarter-model of a reflection-type probe placed over a stack of ten conducting plates is shown in Fig. 3. The inset shows the corresponding experimental probe of identical geometry. The plates had no defect, so it was convenient to use cylindrical symmetry. The screenshot of a solved 2D model depicting the phi-component of surface current density recorded at a time corresponding to the peak amplitude of the pickup signal is shown in Fig. 4. It gives a visual indication of currents that penetrate inside the conducting plates. The maximum current density in the plates was found to be between the driver and the pickup coil.

4.1 Model Verification of Lift-Off Intersection Point

The effect of probe lift-off from the sample surface was studied by increasing the distance between the probe and the plate from the default 0.23 mm up to 2.0 mm. The results are shown in Fig. 5 for 10 plates. All the voltage curves, except the air signal, pass through a common point, called the lift-off intersection (LOI) point. The point has been observed experimentally by some researchers [2, 3]. The models thus provide experimental verification of the LOI point.

Table 1: Specifications of Drivers and Pickup Coils

	Driver	**Pickup Coil**
Length, mm	20.0	1.0
Inner diameter, mm	18.9	5.9
Outer diameter, mm	20.9-23.9	8.2
Number of turns	400-1600	300
AWG	34	44
Resistance, Ω	26.0-122	64.0
Length of ferrite core, mm	20.0-30.0	
Diameter of ferrite core, mm	4.0	
Permeability of ferrite	1500-3100	
Conductivity of ferrite, S/m	0.5	
Conductivity of aluminum, S/m	2.46×10^7	

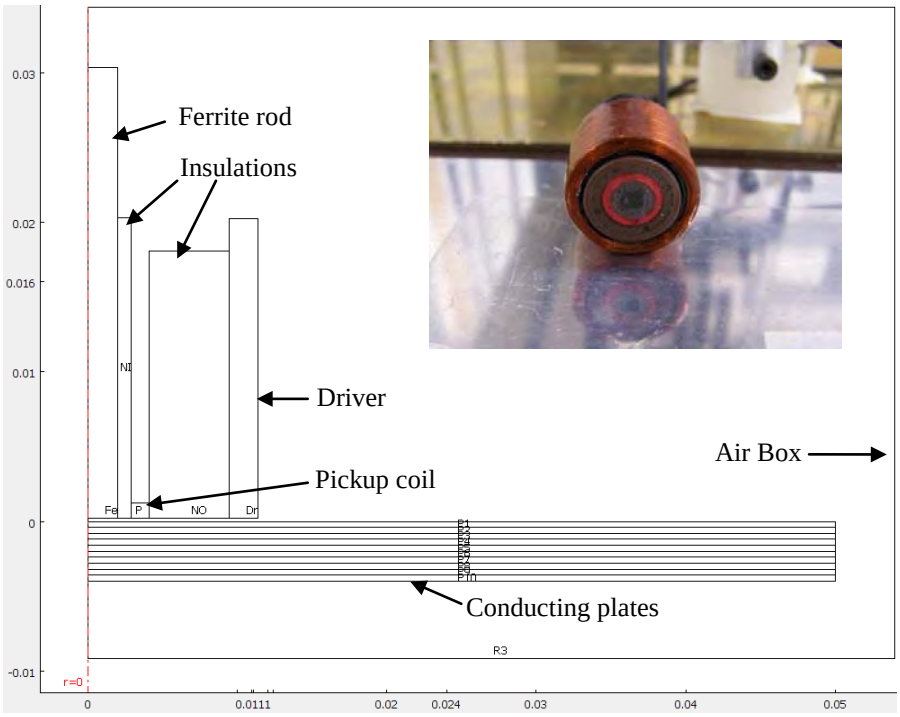

Figure 3. Quarter-section of a 2D finite element model of reflection-type probe placed over a stack of ten conducting plates. The inset shows the experimental probe of identical geometry.

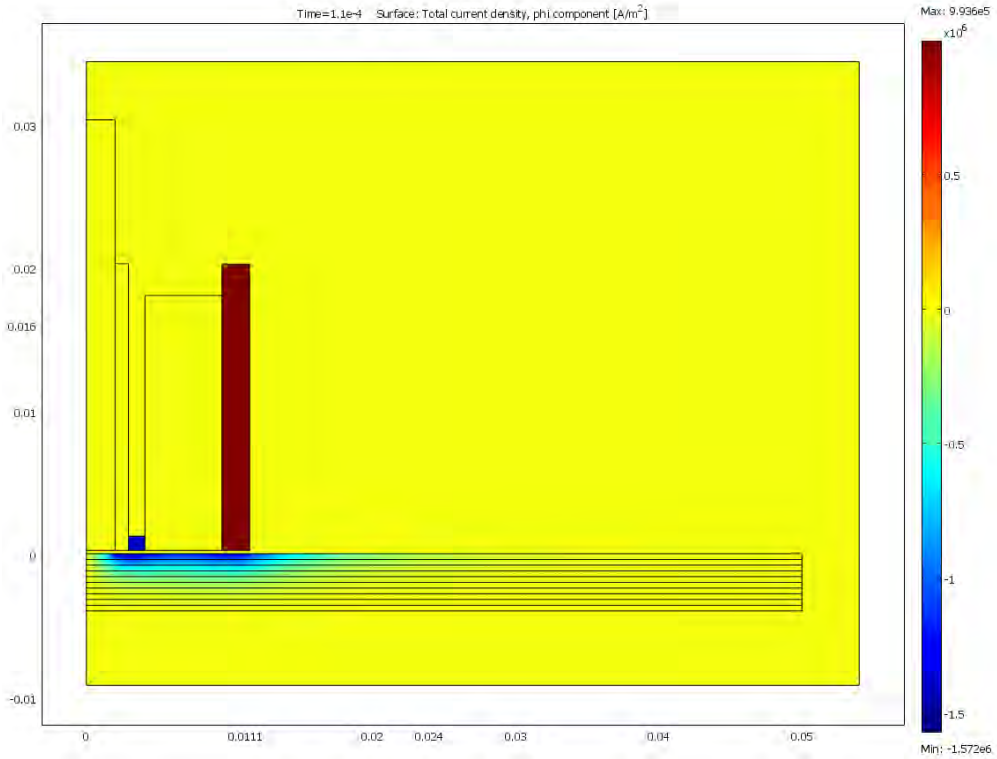

Figure 4. Surface current density (phi-component) near the peak amplitude of the pickup signal, as shown in Fig. 5.

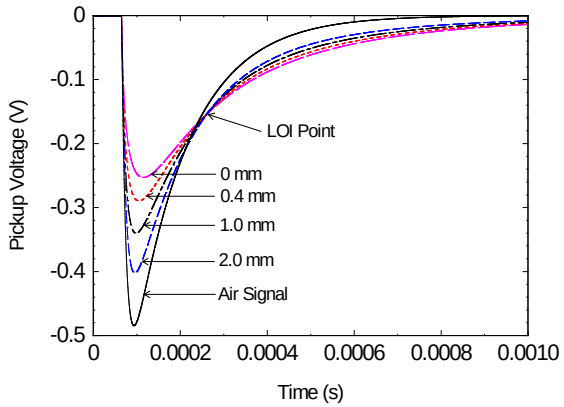

Figure 5. Variation of pickup signal with lift-off for 10 plates.

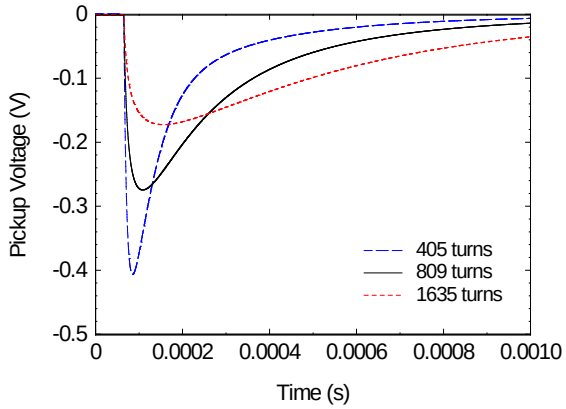

Figure 6. Variation of pickup signal with number of turns of the driver.

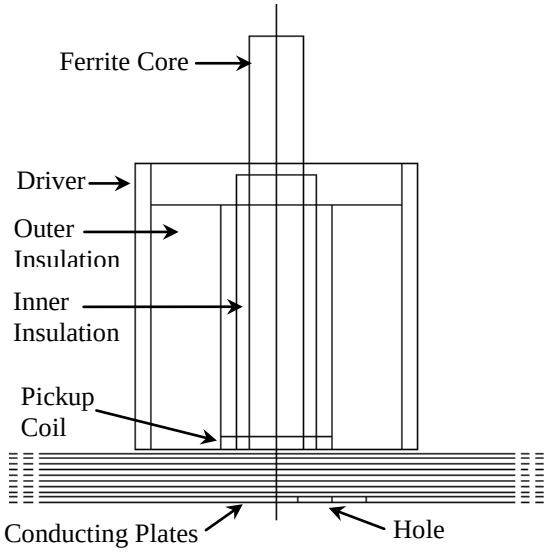

Figure 7. Half-section of a 3D model for nine plates with a hole in the lowermost plate.

4.2 Variation of Pickup Signal with Number of Turns of the Driver

The magnitude and shape of the pickup signal for three different drivers having number of turns equal to 405, 809 and 1635 are shown in Fig. 6. The driver with the least number of turns produces the greatest signal amplitude that decays at the fastest rate. This is attributed to the combined effect of resistance and inductance of the driving circuit with inductance playing a dominant role [8]. The inductance is the minimum for the 405-turns driver. The corresponding smaller relaxation time enhances the rate of growth as well as decay of the driver voltage, thus producing steeper variation in the pickup signal. The 1635-turns driver, on the other hand, has the highest relaxation time and produces the smallest pickup voltage that decays at a slower rate. While a greater voltage is an advantage as it produces larger flux density, a larger relaxation time is vital to detection of deep-lying defects where diffusing currents interact with defects later in time. So the 809-turns driver seems to be a better trade-off between greater relaxation time and larger peak amplitude.

4.3 Effect of Core Length and Permeability

The pickup signals from a driver of coil length 20 mm and three different core lengths (20, 30 and 40 mm) were compared. The signal increased by about 8% for a change in core length from 20 to 30 mm and about 5% from 30 to 40 mm. Longer cores generate flux that can penetrate deeper into the sample and produce greater current density throughout the sample parallel to the surface. However, they make the probe bulky. Models were also produced using core permeability of 1500, 2300 and 3000, but no significant effect on the pickup signal was observed. A ferrite core of length 30 mm and permeability 2300 was selected for this work.

5. 'Defect' Models

The 2D models could not be used to simulate geometries that include 3D localized defects, so the 3D models were produced. However, 3D models put more load on system resources that may lead to crashes, particularly when attempts are made to refine the mesh and increase the total

time. Also, COMSOL3.4 does not allow the use of cylindrical coordinates in 3D, so we used Cartesian coordinates. Despite these problems, the 3D modeling worked well for modeling circular holes. The holes were introduced on one side of the plate, so it was possible to use half models instead of full, which helped to reduce the size of the model. A typical 3D half-model with 9 plates required about 900 MB of memory.

Figure 7 shows a sketch of a vertical cut-out section of a 3D model of a probe. The model dimensions and other parameters were very close to those used in the experiment. However, aluminum plates of reduced size and circular geometry (diameter = 88 mm) were used to utilize the symmetry features of the software as well as to reduce the memory requirement. Since the plate edges were in the far field region, the edge effects were negligible. The finite element mesh of the model had 47,181 tetrahedral elements.

5.1 Effect of Probe Location

Information about the nature, location and severity of a defect is obtained by subtracting the 'no defect', reference, or background signal from the 'defect' signal. Figure 8 shows a reference-subtracted signal from a hole present in a stack of five plates along with the corresponding experimental signal. The reference-subtracted signal shows two peaks of different magnitudes and opposite polarity with the smaller peak occurring later in time. The amplitudes of these peaks are affected by the change in position of the probe with respect to the defect center. FE modeling has revealed that, for the probe dimensions used in the present work, the maximum signal amplitude would occur when the outer edge of the pickup coil coincided with the center of the hole. This corresponded to the center-to-center distance of 4 mm between the hole and the probe, as shown in Fig. 9. The signal strength decreased when the probe was shifted on either side of the hole center. The models used in the work correspond to this particular position of the probe. Two different views of a solved 3D model depicting x-component of the surface current density are shown in Fig. 10. Differences in the current density in the vicinity of the hole are evident.

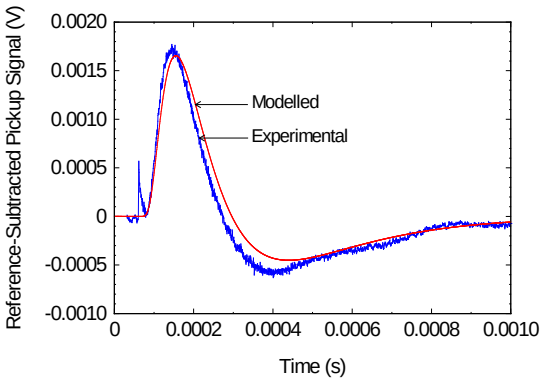

Figure 8. Reference-subtracted signal from a 'defect' model with five plates.

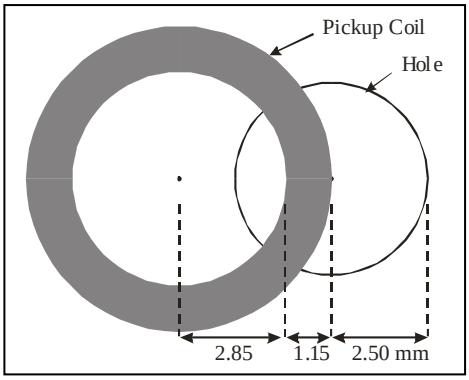

Figure 9. Position of the pickup coil relative to the hole that produced the strongest signal.

5.2 Effect of Sample Thickness

The thickness of the sample was varied by increasing the number of plates, with the hole always present in the lowermost plate. The variation of reference-subtracted signal with change in thickness (or number of plates) of the multilayer structure is shown in Fig. 11. The amplitude of both the peaks decreased and the peaks shifted to later times with increase in thickness. The existence of two peaks and the shifts of the peaks are indicative of diffusion wave phenomena, where the second peak can be associated with the secondary induced currents that have greater depth-of-penetration. Thus the size and position of the peaks can provide useful information about the location of defects within the multilayer structures.

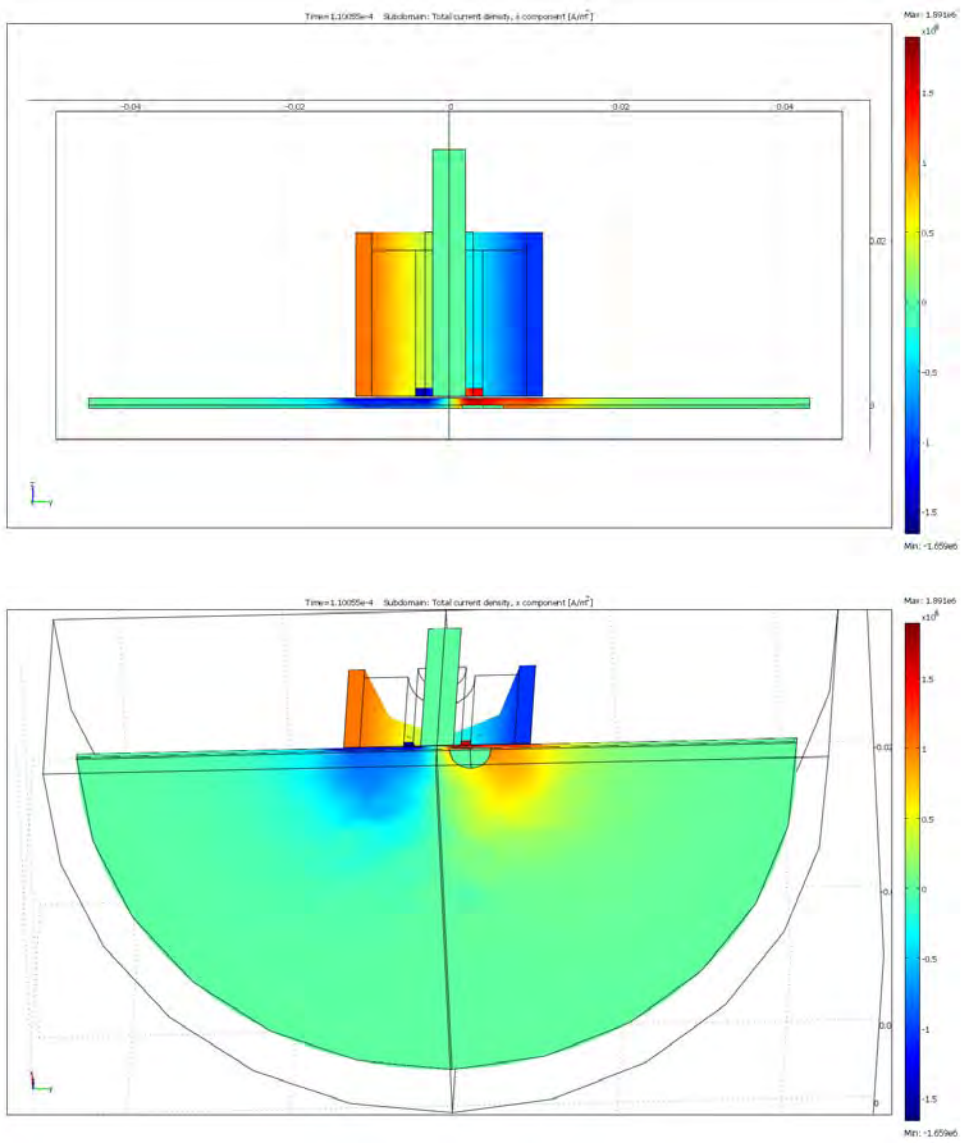

Figure 10. Views of the solved model showing surface current density along the x direction (normal to the plane of the paper). The hole is visible in the lowermost figure.

6. Conclusion

The finite element modeling using COMSOL Multiphysics software succeeded in simulating the transient eddy current response in multilayered aluminum structures containing circular defects. It verified some known experimental results, such as the existence of the lift-off intersection point, and contributed to the investigation of different probe configurations and determination of optimum probe parameters. The modeled results are in good agreement with experimental observations.

7. Acknowledgement

The authors thank Mr. Kevin Wannamaker for technical assistance. This work is supported by the Natural Sciences and Engineering Research Council of Canada, and the Academic Research Program and the Aerospace Research Advisory Committee at the Royal Military College of Canada.

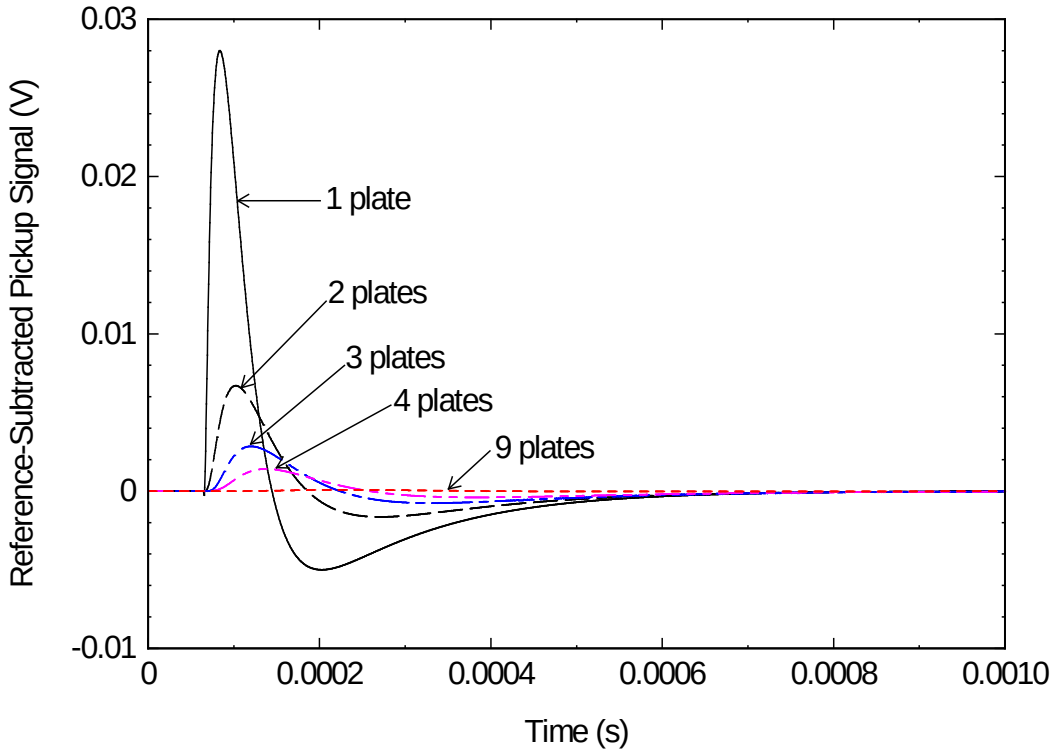

Figure 11. Variation of reference-subtracted pickup signal with number of plates.

8. References

1. M. Gibbs and J. Campbell, "Pulsed Eddy Current Inspection of Cracks under Installed Fasteners," *Mater. Eval*., **49**, pp. 51-59 (1991).
2. S. Giguere and J. M. S. Dubois, "Pulsed Eddy Current: Finding Corrosion Independently of Transducer Lift-off," in *Review of Progress in QNDE*, **19**, edited by D. O. Thompson and D. E. Chimenti, AIP Conference Proceedings vol. 615, American Institute of Physics, Melville, NY, pp. 449-456 (2000).
3. S. Giguere, B.A. Lepine and J.M.S Dubois, "Pulsed Eddy Current Technology: Characterizing Material Loss with Gap and Lift-off Variations," in *Review of Progress in QNDE*, **20**, *op. cit*., pp. 119-129 (2001).
4. Y. A. Plotnikov, S. C. Nath and C. W. Rose, "Defect Characterization in Multilayered Conductive Components with Pulsed Eddy Current," in *Review of Progress in QNDE*, **21**, *op. cit.*, pp. 1976-1983 (2002).
5. T. W. Krause, C. Mandache, and J. H. V. Lefebvre, "Diffusion of Pulsed Eddy Currents in Thin Conducting Plates," in *Review of Progress in QNDE*, **27**, *op. cit.*, pp. 368-375 (2008).
6. J. R. Bowler, D. J. Harrison, "Measurement and Calculation of Transient Eddy Currents in Layered Structures," in *Review of Progress in QNDE*, **11**, *op. cit.*, pp. 241-248 (1992).
7. J. R. Bowler, Pulsed Eddy Current Interaction with Subsurface Cracks," in *Review of Progress in QNDE*, **18**, *op. cit.*, pp. 477-483 (1999).
8. T. J. Cadeau and T.W. Krause, "Pulsed Eddy Current Probe Design Based on Transient Circuit Analysis," in *Review of Progress in QNDE*, **28**, *op. cit.*, pp. 327-334 (2009).
9. V. K. Babbar, P. V. Kooten, T. J. Cadeau and T. W. Krause, "Finite Element Modeling of Pulsed Eddy Current Signals from Conducting Cylinders and Plates," *in Review of Progress in QNDE*, **28**, *op. cit.*, pp. 311-318 (2009).